

An improved generalized AMBER force field (GAFF) for urea

Gül Altınbaş Özpınar · Wolfgang Peukert · Timothy Clark

Received: 8 December 2009 / Accepted: 22 December 2009 / Published online: 17 February 2010
© Springer-Verlag 2010

Abstract We describe an improved force field parameter set for the generalized AMBER force field (GAFF) for urea. Quantum chemical computations were used to obtain geometrical and energetic parameters of urea dimers and larger oligomers using AM1 semiempirical MO theory, density functional theory at the B3LYP/6-31G(d,p) level, MP2 and CCSD ab initio calculations with the 6-311++G(d,p), aug-cc-pVDZ, aug-cc-pVTZ, and aug-cc-pVQZ basis sets, and with the CBS-QB3 and CBS-APNO complete basis set methods. Seven different urea dimer structures were optimized at the MP2/aug-cc-pVDZ level to obtain

accurate interaction energies. Atomic partial charges were calculated at the MP2/aug-cc-pVDZ level with the restrained electrostatic potential (RESP) fitting approach. The interaction energies computed with these new RESP charges in the force field are consistent with those obtained from CCSD and MP2 calculations. The linear dimer structure calculated using the force field with modified geometrical parameters and the new RESP charge set agrees well with available experimental data.

Keywords GAFF · Force field parameters · Urea · Urea dimers · Urea crystal

Electronic supplementary material The online version of this article (doi:10.1007/s00894-010-0650-7) contains supplementary material, which is available to authorized users.

G. A. Özpınar · T. Clark (✉)
Computer-Chemie-Centrum and Interdisciplinary
Center for Molecular Materials,
Friedrich-Alexander Universität Erlangen-Nürnberg,
Nägelsbachstr. 25,
91052 Erlangen, Germany
e-mail: Tim.Clark@chemie.uni-erlangen.de

G. A. Özpınar · W. Peukert · T. Clark
Engineering of Advanced Materials,
University of Erlangen-Nürnberg,
Nägelsbachstr. 49b,
91052 Erlangen, Germany

G. A. Özpınar
Department of Chemistry, Faculty of Arts and Sciences,
University of Marmara,
Göztepe Campus,
34722 Istanbul, Turkey

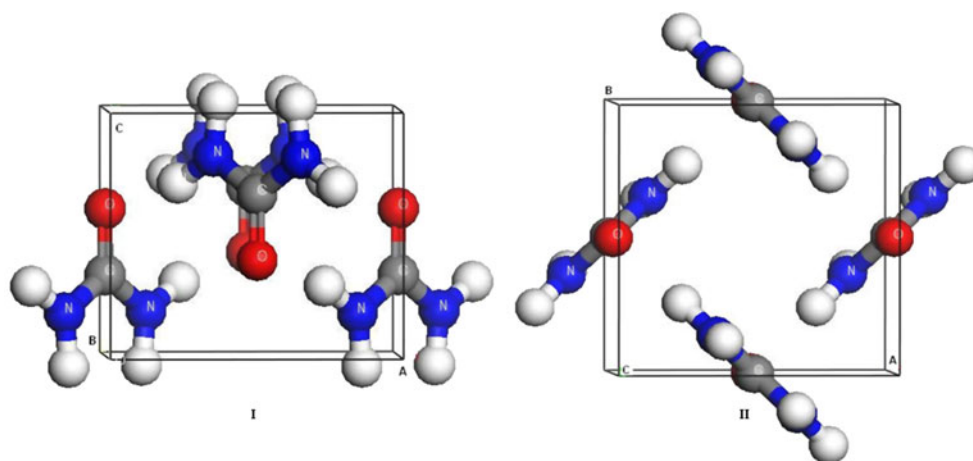
W. Peukert
Lehrstuhl für Feststoff- und Grenzflächenverfahrenstechnik,
Cauerstraße 4,
91058 Erlangen, Germany

Introduction

Urea and substituted ureas are an important class of organic molecules since they are used in many areas, such as the agricultural, pharmaceutical, chemical, and medical industries. Urea has been used as a powerful protein denaturant, a stabilizer in nitrocellulose explosive, a cloud-seeding agent, a flame-proofing agent, and a nitrogen source [1]. Its interesting nonlinear optical properties [2], ability to form clathrates [3] and transition-metal complexes [4], and the relative simplicity of its crystal structure make urea one of the most interesting crystalline materials. X-ray and neutron diffraction studies of its crystal structure have been performed by several authors [5–13]. These early studies agreed on the space group, unit cell, and that its oxygen atom accepts four hydrogen bonds N–H...O in the crystal structure. Figure 1 shows the unit cell structure of crystalline urea.

There have been many theoretical studies of the electronic [14–19] and energetic [20, 21] properties of urea. Molecular dynamics simulations [22–25] of its

Fig. 1 The unit cell of urea crystal. *I* and *II* are projections of the structure down the *a*-axis and along the *c*-axis, respectively. The space group is $P4_21m$ and the unit cell dimensions are $a=b=5.565$ and $c=4.684$ Å [12]



interactions with water and organic molecules have also been used in order to understand the growth of urea crystals from aqueous solution. However, the reported data on interactions and hydrogen bond formation differ significantly because of the different empirical force fields used [26, 27], which emphasizes the importance of using an accurate and consistent set of parameters for urea. This is important because urea is quite unusual in that it contains four hydrogen-bond donors and that its carbonyl oxygen accepts four hydrogen bonds in the crystal structure. Etter [28] reviewed hydrogen-bond patterns of organic compounds, especially ureas, and was able to establish rules for hydrogen bonding in crystals, co-crystals and clathrates. Hence, in this work, we present a refined force field based on the generalized AMBER force field (GAFF) [29]. Geometrical parameters were produced for urea systems

using semiempirical, density functional and high level ab initio calculations. Since an accurate description of urea dimer formation is essential in order to be able to describe urea nucleation, aggregation and behavior as a clathrate host, we have investigated the structures and energies of different urea oligomers. In order to fit urea–urea interactions obtained from high level ab initio calculations, we have generated a set of charges for each dimer and compared the interaction energies after energy minimization with force fields using these charge sets.

Computational methods

Semiempirical computations were carried out using the VAMP 10.0 [30] program, and all other calculations were

Fig. 2 Potential energy surface of urea. Relative energies at the B3LYP/6-31G**, B3PW95/D95** [20] (*bold*), MP2/D95** [18] (*in parentheses*), and MP2/6-31G* [56] (*italics*) levels

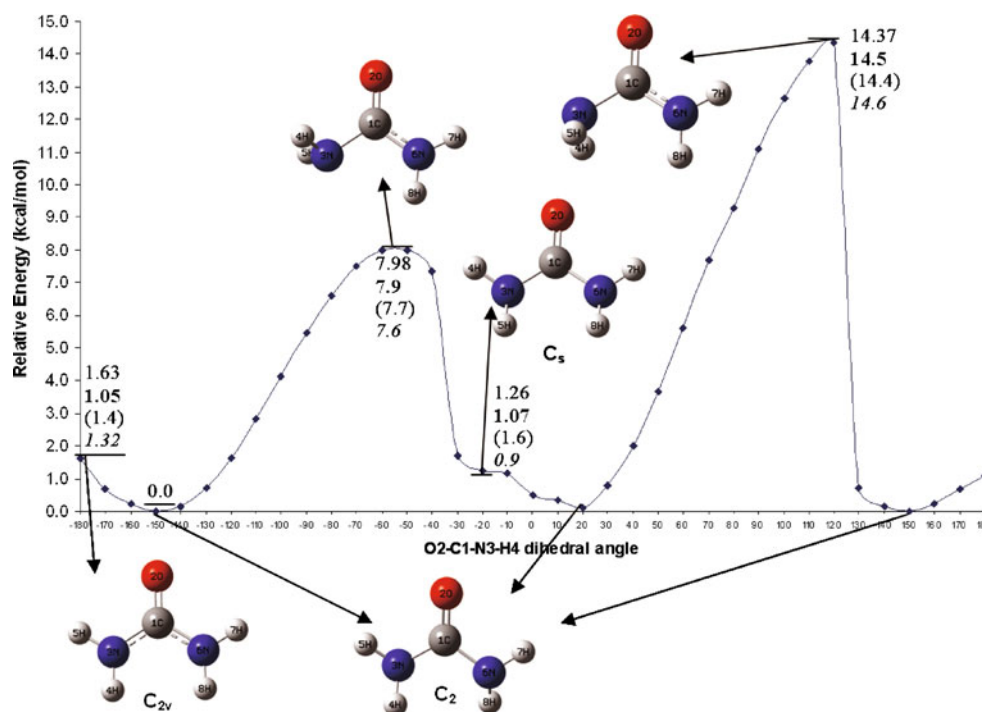


Table 1 Relative total energies (kcal mol⁻¹) for urea conformers

Computational method	$\Delta E(C_{2v}-C_2)$
AM1	0.87
HF/6-31G(d)	1.57 ^a
HF/D95**	1.29 ^a
HF/6-311+G(3df,2p)	0.58 ^a
B3PW91/D95**	1.46 ^a
B3PW91/6-311+G(3df,2p)	0.59 ^a
B3LYP/6-31G(d,p)	1.63
B3LYP/6-311+G*	1.20 ^b
MP2/D95**	2.49 ^a
MP2/6-31G*	1.32 ^c
MP2/6-311++G(d,p)	2.75
MP2/6-311+G(3df,2p)	1.19 ^a
MP2/aug-cc-pVDZ	1.58
MP2/aug-cc-pVTZ	1.42
MP2/aug-cc-pVQZ	1.22
CCSD/aug-cc-pVDZ	0.94
CCSD/aug-cc-pVTZ	0.70
CCSD(T)/aug-cc-pVDZ	0.94 ^d
CCSD(T)/aug-cc-pVTZ	0.56 ^e
CBS-QB3	1.29
CBS-APNO	1.12

^a Taken from [20]

^b Taken from [18]

^c Taken from [56]

^d Single-point energy at CCSD/aug-cc-pVDZ geometry

^e Single-point energy at CCSD/aug-cc-pVTZ geometry

performed using the Gaussian 03 [31] suite of programs. The geometry optimizations of the urea monomer were performed with CCSD [32–34], CCSD(T), MP2 [35], B3LYP [36, 37], AM1 [38] and complete basis set [39–41] (CBS) methods. The aug-cc-pVDZ, aug-cc-pVTZ, aug-cc-pVQZ [42–46], 6-311++G(d,p) [47–49], and 6-31G(d,p) [50, 51] basis sets were used. Urea clusters were built by repeating the unit cell in the A, B, and C directions. For the cluster optimizations, AM1 and B3LYP/6-31G(d,p) were chosen as compromises between accuracy and computational cost.

The different urea dimer structures were optimized at the MP2/aug-cc-pVDZ level and frequency calculations at the same level were carried out within the harmonic approximation to characterize the dimeric stationary points. The counterpoise (CP) correction method of Boys and Bernardi [52] was used in order to correct for basis set superposition error (BSSE) in the dimers. Single-point calculations at the MP2/aug-cc-pVTZ and CCSD/aug-cc-pVDZ levels were also performed.

The AMBER [53] program was used for energy minimizations with GAFF and the modified force field.

Table 2 Geometrical parameters (bond distances in Å and angles in °) for urea

	C=O		C-N		N-H4		N-H5		∠N-C-N		∠N-C-O		∠H4-N-C		∠H5-N-C		∠H-N-H	
	C ₂	C _{2v}	C ₂	C _{2v}	C ₂	C _{2v}	C ₂	C _{2v}	C ₂	C _{2v}	C ₂	C _{2v}	C ₂	C _{2v}	C ₂	C _{2v}	C ₂	C _{2v}
AM1	1.256	1.258	1.403	1.389	0.994	0.988	0.991	0.984	120.1	120.3	120.0	119.8	118.6	122.9	114.8	117.3	115.7	119.8
B3LYP/6-31G**	1.221	1.224	1.390	1.377	1.011	1.006	1.010	1.005	113.7	114.9	123.1	122.5	117.4	124.3	112.3	116.6	113.7	119.1
CCSD/aug-cc-pvdz	1.223	1.228	1.395	1.380	1.014	1.008	1.014	1.008	113.6	114.9	123.2	122.5	116.0	123.4	112.2	117.1	113.7	119.5
CCSD/aug-cc-pvtz	1.212	1.216	1.384	1.369	1.006	1.000	1.006	1.001	113.8	115.0	123.1	122.5	116.7	123.4	112.7	117.0	114.2	119.5
CBS-QB3	1.214	1.217	1.389	1.376	1.009	1.004	1.009	1.004	113.6	114.8	123.2	122.6	117.6	124.1	112.9	116.8	114.4	119.1
CBS-APNO	1.212	1.216	1.394	1.377	1.010	1.003	1.009	1.003	112.7	114.3	123.6	122.9	115.0	123.7	111.7	117.0	113.0	119.3
MP2/aug-cc-pvdz	1.230	1.233	1.394	1.381	1.014	1.008	1.014	1.009	113.5	114.8	123.2	122.6	116.5	123.6	112.4	117.0	114.0	119.4
MP2/aug-cc-pvtz	1.219	1.222	1.384	1.371	1.007	1.001	1.007	1.002	113.6	114.8	123.2	122.6	117.1	123.6	112.8	117.0	114.5	119.5
MP2/aug-cc-pvqz	1.216	1.219	1.381	1.368	1.005	1.000	1.005	1.001	113.7	114.8	123.1	122.6	117.5	123.5	113.1	117.0	114.8	119.5
MP2/6-311++G**	1.218	1.221	1.391	1.377	1.010	1.004	1.010	1.005	113.1	114.5	123.4	122.8	116.2	123.8	112.4	117.0	113.8	119.2
GAFF parameters	-	1.214	-	1.345	-	1.009	-	1.009	-	111.7	-	122.0	-	-	118.5	-	-	117.8
Cornell et al. [57]	-	1.250	-	1.383	-	1.010	-	1.010	-	118.6	-	120.9	-	-	120.0	-	-	120.0
Exp.	-	1.262 ^a	-	1.335 ^a	-	0.988 ^b	-	0.995 ^b	-	118.0 ^a	-	121.0 ^a	-	-	118.1 ^b	-	-	122.0 ^b
	-	1.243 ^b	-	1.351 ^b	-	1.046 ^c	-	1.046 ^c	-	117.0 ^b	-	121.5 ^b	-	-	120.0 ^c	-	-	119.0 ^c

^a Taken from [7]

^b Taken from [8]

^c Taken from [9]

Atom types were assigned using the default GAFF parameters. A set of restrained electrostatic potential (RESP) atomic charges [54] were calculated at the MP2/aug-cc-pVDZ level using Gaussian 03. The RESP charges for hydrogen atoms on the NH₂ groups were constrained to be equal. The fitting procedure was performed using the single-conformation, two-stage RESP fitting approach. Dimer geometries were optimized with 1,000 steps of steepest-descent minimization.

Results

Urea monomer

The urea molecule exhibits C_{2v} symmetry in the solid state. Therefore, the experimental values for its geometrical parameters in the literature refer to the C_{2v} structure. However, the most stable conformation in the gas phase has C₂ symmetry. Microwave spectra [55] of urea have confirmed that the hydrogen atoms bonded to each nitrogen atom are located in *anti*-configurations to each other in the gas phase. Figure 2 shows the calculated potential energy surface of urea. Relative energies for the urea conformers are listed in Table 1, which shows that the stabilities of urea conformers depend strongly on the computational method used. Increasing the size of the basis set decreases the relative energy of the C_{2v} structure by 0.2–1.1 kcal mol⁻¹. Interestingly, AM1 gives relative energies very close to those obtained with CCSD/aug-cc-pVDZ and CCSD(T)/aug-cc-pVDZ.

Geometrical parameters of the two urea conformers are shown in Table 2. The change of symmetry from C₂ to C_{2v} causes the C–N and N–H bonds to shorten and the C=O bond to lengthen. The N–C–N, H–N–C, and H–N–H bond angles increase and the N–C–O bond angle narrows.

Remarkably, the AM1-calculated C=O bond length and N–C–N bond angle agree best with experiment. All methods overestimate the C–N bond length. The H–N bond lengths are shorter than those of Andrew et al. [8], but the AM1 bond length is close to the experimental one published by Worsham et al. [7]. The H5–N–C bond angles are underestimated and the H4–N–C bond angles overestimated by all the methods investigated. In the existing GAFF parameters [29], the C–N bond length and the H–C–N bond angle agree with the experimental data and the C=O distance is consistent with the data obtained from high-level calculations. However, the N–C–N angle is quite narrow compared to both the experimental and high-level theoretical values. In an alternative force field parameter set generated by Cornell et al. [57], the C=O distance is close to the AM1 and experimental values and the C–N distance agrees with those obtained from the computations with CCSD/aug-cc-pVDZ and MP2/aug-cc-pVDZ. Generally, the bond angles in this parameterization agree better with the experimental data than either the original GAFF force field or our quantum mechanically calculated values.

The experimental dipole moment of urea has been estimated to be 3.83 D [55] in the gas phase, 4.2 D [58] in aqueous solution and 4.66 D [59] in the solid state. Figure 3 shows comparisons of computed urea dipole moments with experimental data. The AM1 and B3LYP dipole moments for the C_{2v} structure are very close to the experimental ones found in solution. The CCSD/aug-cc-pvtz and CBS-APNO methods agree best with the experimental value in the solid state.

Urea dimers

In order to be able to describe the formation of the urea dimer correctly, we have optimized seven different urea

Fig. 3 Comparison of computed urea dipole moments (Debye) with experimental data

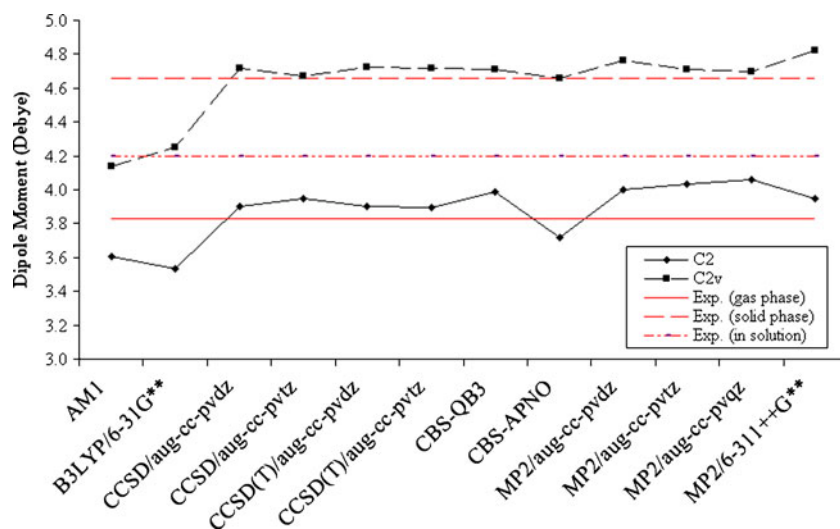
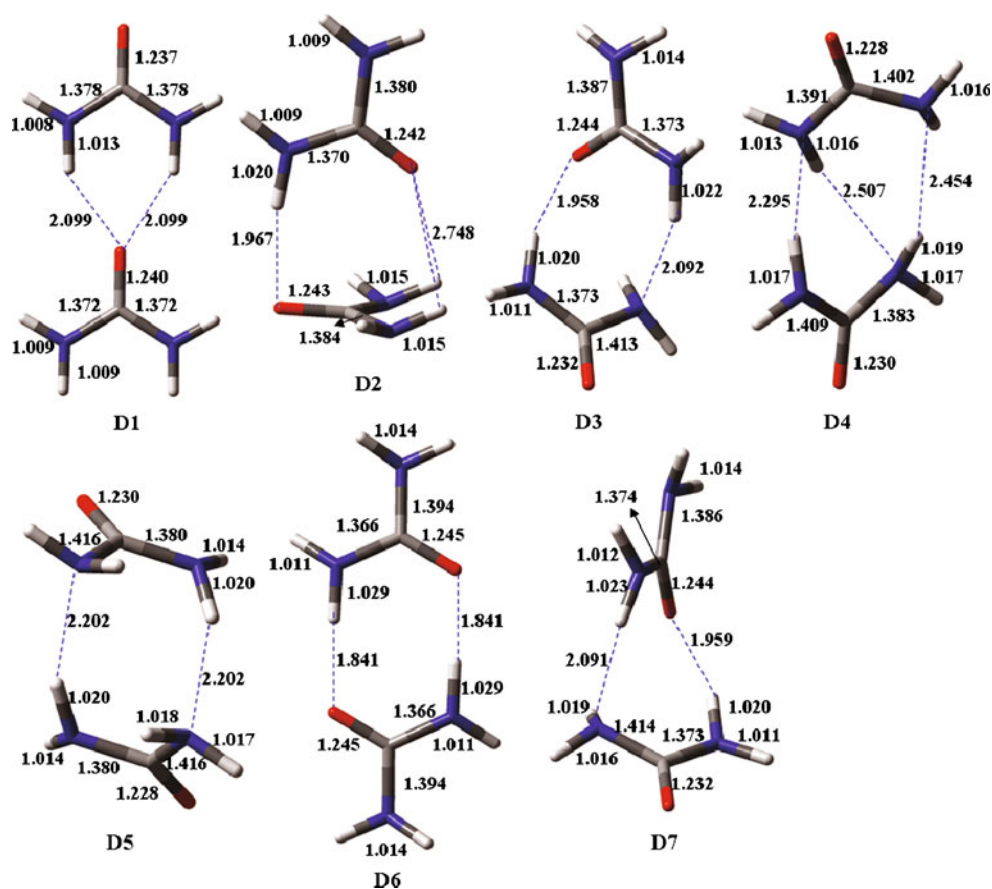


Fig. 4 Urea dimer structures optimized at the MP2/aug-cc-pVDZ level: red, O; gray, C; blue, N; white, H; distances in Å). The exact geometries are given in the “Electronic supplementary material”



dimer structures at the MP2/aug-cc-pVDZ level. The optimized geometries are shown in Fig. 4. **D1** is the linear “head-to-tail” dimer found in the crystal structure and **D6** is cyclic dimer that is most stable in the gas phase. The C=O bond distance lengthens from 1.23 to 1.24 Å because of

C=O...N–H hydrogen bonding, whereas the C–N single bond shortens from 1.39 to 1.37 Å, in agreement with experiment. Relative energies are listed in Table 3.

All methods agree on the stability order **D6**>**D3**≈**D7**>**D5**~**D2**>**D1**>**D4**. The BSSE correction does not affect the

Table 3 Relative energies (kcal mol⁻¹) (*E*: total energy, *E*_{ZPE}: zero-point corrected energy, and *E*_{BSSE}: counterpoise corrected energy) and the number of imaginary frequencies (NIMAG) of urea dimers

	<i>E</i>	<i>E</i> _{ZPE}	<i>E</i> _{BSSE}	<i>E</i> ^a	<i>E</i> ^b	<i>E</i> ^c	<i>E</i> ^d	<i>E</i> ^e	<i>E</i> ^f	NIMAG
D1	7.56	5.18	6.74	7.39	7.50	7.94	5.01	5.12	5.56	5
D2	5.85	4.51	6.00	6.18	5.72	6.23	4.83	4.37	4.89	2
D3	1.75	1.92	2.10	2.22	2.06	2.43	2.39	2.22	2.60	0
D4	7.47	7.54	7.57	8.25	7.63	8.37	8.32	7.70	8.44	0
D5	5.06	5.55	5.72	6.16	5.50	6.37	6.65	5.99	6.86	0
D6	0.00	0.00	0.00	0.00	0.00	0.00	0.00	0.00	0.00	0
D7	1.81	1.99	2.15	2.25	2.09	2.43	2.43	2.27	2.62	0

^a MP2/aug-cc-pVTZ// MP2/aug-cc-pVDZ energy

^b CCSD/ aug-cc-pVDZ// MP2/aug-cc-pVDZ energy

^c CCSD(T)/ aug-cc-pVTZ// MP2/aug-cc-pVDZ energy

^d MP2/aug-cc-pVTZ// MP2/aug-cc-pVDZ energy corrected with the MP2/aug-cc-pVDZ zero-point vibrational energy

^e CCSD/ aug-cc-pVDZ// MP2/aug-cc-pVDZ energy corrected with the MP2/aug-cc-pVDZ zero-point vibrational energy

^f CCSD(T)/ aug-cc-pVTZ// MP2/aug-cc-pVDZ energy corrected with the MP2/aug-cc-pVDZ zero-point vibrational energy

relative MP2/aug-cc-pVDZ energies significantly, as might be expected for urea, which is relatively polar [60–62].

Urea oligomers

In order to see how the bond distances change as the number of urea molecules increases, we built urea clusters containing up to 160 urea molecules and optimized their geometries with AM1 and at the B3LYP/6-31G(d,p) level.

The optimized urea clusters are shown in Figs. 5 and 6. As the number of molecules in the cluster increases, the length of the single bond C–N shortens and the C=O double bond lengthens (Table 4) because of the hydrogen bonding. This explains the differences between the bond distances and angles calculated experimentally and theoretically. As the size of the system increases, AM1 begins to overestimate the C=O and C–N distances. However, B3LYP gives more reasonable values for these distances. The N–H bond

Fig. 5 AM1 (left column) and B3LYP (right column) optimized geometries of urea clusters ($n=4, 7, 12,$ and 24). Dashed lines show hydrogen bonding: red, O; gray, C; blue, N; white, H. The exact geometries are given in the “Electronic supplementary material”

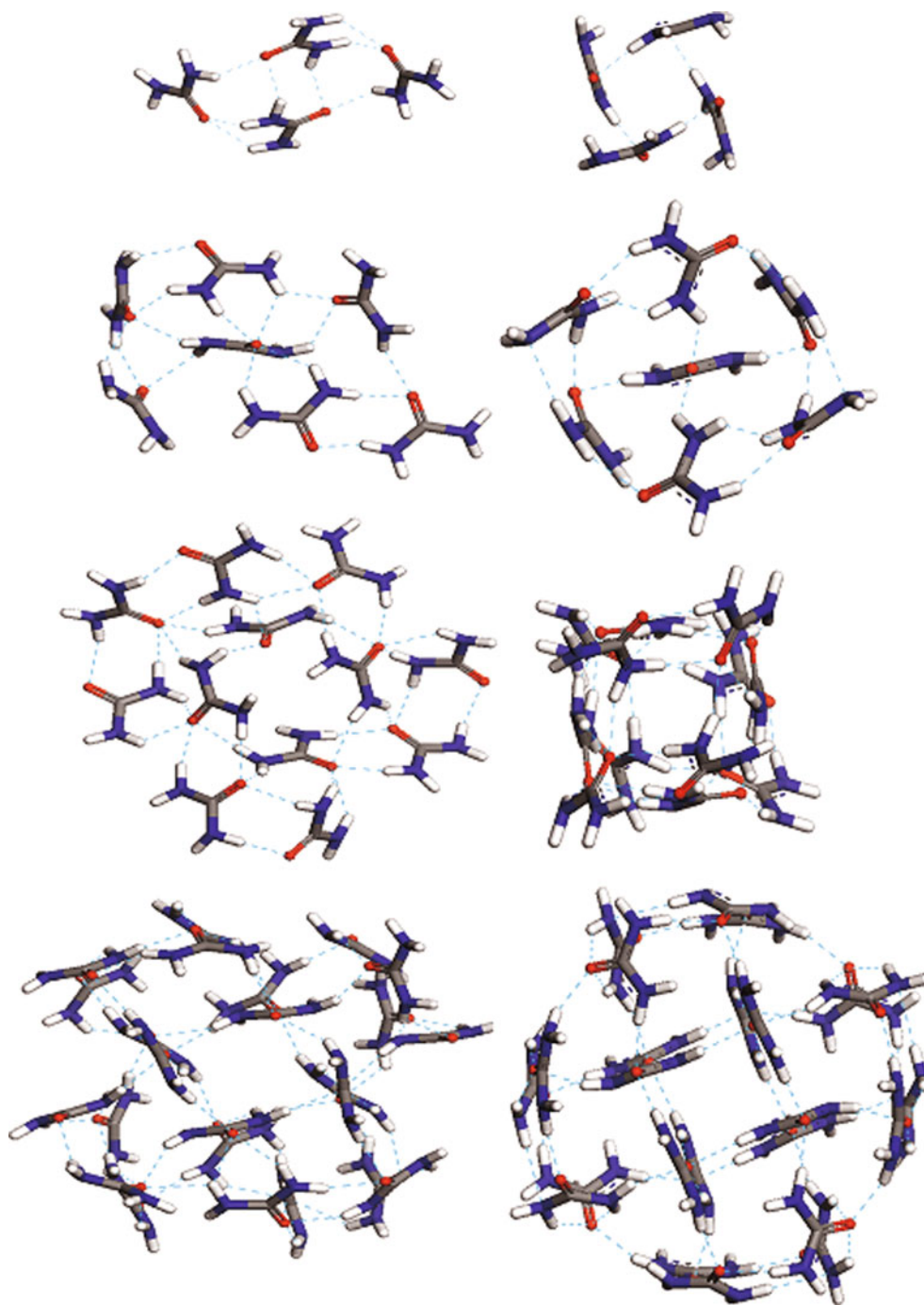
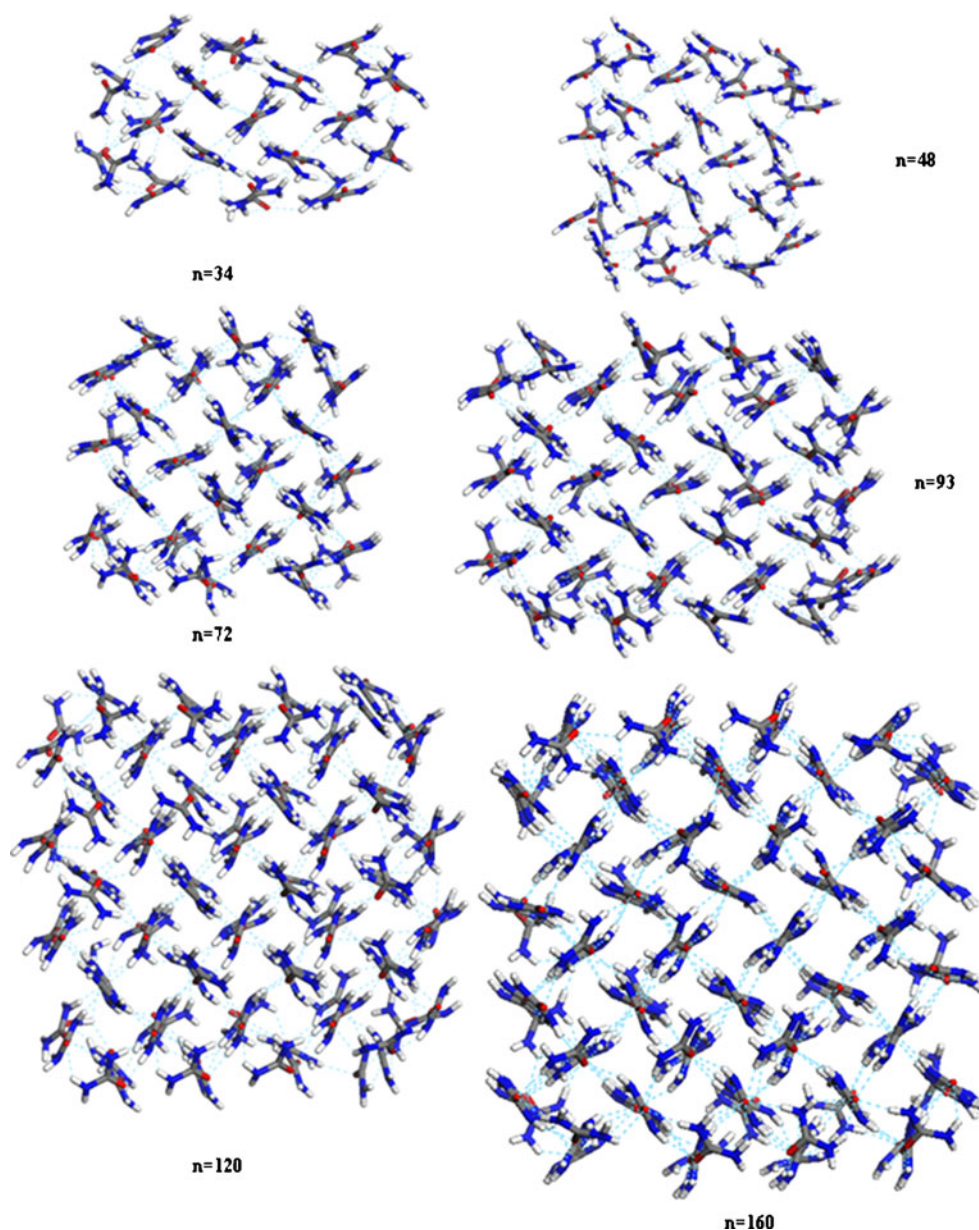


Fig. 6 AM1 optimization results for urea clusters. *Dashed lines* show hydrogen bonds: *red*, O; *gray*, C; *blue*, N; *white*, H. The exact geometries are given in the “Electronic supplementary material”



distances did not change on increasing the size of the clusters. The deviations of the mean C–N and C=O bond lengths from the experimental values are +0.046 and +0.020 Å, respectively, for AM1 (160 molecules), and +0.020 and +0.001 Å for B3LYP (24 molecules). The O–C–N bond angle shrinks and the N–C–N, C–N–H and H–N–H bond angles widen as the size of the cluster increases (Table 5).

A plot of the calculated binding energies of the urea clusters is shown in Fig. 7. The results can be fitted to the following linear equations to allow us to estimate the lattice energy of the urea crystal at AM1 and B3LYP/6-31G(d,p).

$$E_{AM1} = 35.3 - 11.25n \quad (1)$$

$$E_{B3LYP} = 32.2 - 19.48n \quad (2)$$

The predicted lattice energies (-11.3 and -19.5 kcal mol $^{-1}$ for AM1 and B3LYP/6-31G(d,p), respectively) are smaller than the experimental values (taken here to be minus the sublimation energy) of -20.95 ± 0.21 [63] and -23.6 kcal mol $^{-1}$ [64]. These deviations can be expected because neither AM1 nor B3LYP can reproduce the stabilizing dispersion interaction, although the magnitude of the deviation for AM1 also suggests that it underestimates the strengths of the intermolecular hydrogen bonds and Coulomb interactions. The relatively good B3LYP result suggests that dispersion does not play a major role.

Table 4 Mean values of optimized bond distances (Å) for some urea clusters. Maximum and minimum values are given in parentheses

Number of molecules	C–N		C=O		N–H	
	AMI	B3LYP	AMI	B3LYP	AMI	B3LYP
4	1.398	1.359	1.264	1.242	0.995 (1.003–0.986)	1.014 1.012 1.008 1.021
7	1.394 1.394 (1.403–1.384)	1.390 1.368 (1.395–1.357)	1.269 1.267 (1.270–1.264)	1.238 1.258 1.247 1.243	0.995 (1.003–0.986)	1.014 (1.027–1.007)
12	1.393 (1.403–1.377)	1.364 (1.376–1.356)	1.269 (1.277–1.264)	1.253 (1.262–1.237)	0.995 (1.003–0.988)	1.016 (1.028–1.008)
24	1.391 (1.401–1.377)	1.363 (1.388–1.349)	1.270 (1.274–1.266)	1.254 (1.262–1.234)	0.995 (1.003–0.988)	1.015 (1.030–1.007)
34	1.391 (1.408–1.379)	–	1.271 (1.275–1.266)	–	0.995 (1.003–0.987)	–
48	1.391 (1.406–1.379)	–	1.271 (1.276–1.266)	–	0.995 (1.003–0.988)	–
72	1.390 (1.408–1.377)	–	1.272 (1.276–1.267)	–	0.995 (1.001–0.986)	–
93	1.389 (1.407–1.375)	–	1.272 (1.277–1.267)	–	0.995 (1.001–0.987)	–
120	1.389 (1.407–1.379)	–	1.272 (1.277–1.267)	–	0.995 (1.003–0.987)	–
160	1.389 (1.408–1.374)	–	1.273 (1.276–1.267)	–	0.995 (1.001–0.987)	–
Exp.	1.335 or 1.351	1.262 or 1.243	0.988 or 0.995 or 1.046			

Table 5 Mean values of optimized bond angles (°) for urea clusters. Maximum and minimum values are given in parentheses

Number of molecules	O–C–N		N–C–N		C–N–H		H–N–H	
	AMI	B3LYP	AMI	B3LYP	AMI	B3LYP	AMI	B3LYP
4	119.59 (120.3–118.9)	121.7	120.58	120.58	116.8 (119.4–114.8)	119.5 117.7 113.6 110.3	115.95 (117.1–114.7)	118.2 110.6
7	119.50 (120.5–118.9)	122.5 (125.0–120.5)	120.94 (121.6–120.2)	115.9 114.5	117.03 (121.5–113.6)	117.03 (121.3–112.6)	115.87 (119.0–113.5)	117.41 (120.0–114.4)
12	119.43 (120.3–118.4)	121.5 (123.5–120.1)	121.06 (121.9–120.2)	116.9 (118.8–115.4)	117.18 (122.3–113.4)	117.1 (119.5–112.9)	116.22 (118.8–113.8)	116.6 (119.4–113.6)
24	119.48 (120.4–118.6)	121.7 (123.6–120.6)	120.95 (121.6–120.5)	116.5 (118.4–114.4)	117.43 (121.9–113.9)	117.8 (121.3–113.7)	116.64 (119.4–113.2)	116.6 (119.2–113.6)
34	119.48 (120.6–118.5)	–	120.94 (121.7–120.3)	–	117.48 (121.4–112.7)	–	116.78 (119.3–112.5)	–
48	119.44 (120.5–118.4)	–	121.03 (121.6–120.3)	–	117.36 (121.8–112.7)	–	116.56 (119.8–112.5)	–
72	119.43 (120.6–118.4)	–	121.08 (121.9–120.2)	–	117.64 (122.1–113.4)	–	116.98 (120.1–113.0)	–
93	119.43 (120.6–118.4)	–	121.08 (121.8–120.5)	–	117.67 (122.0–112.7)	–	117.07 (120.1–112.6)	–
120	119.43 (120.5–118.5)	–	121.08 (121.9–120.4)	–	117.66 (122.1–112.5)	–	117.04 (120.1–112.9)	–
160	119.39 (120.5–118.4)	–	121.16 (121.9–120.5)	–	117.73 (122.1–113.3)	–	117.14 (120.0–113.0)	–
Exp.	121.0 or 121.5	118.0 or 117.0	119.8 or 118.1 or 120.0	122.0 or 119.0				

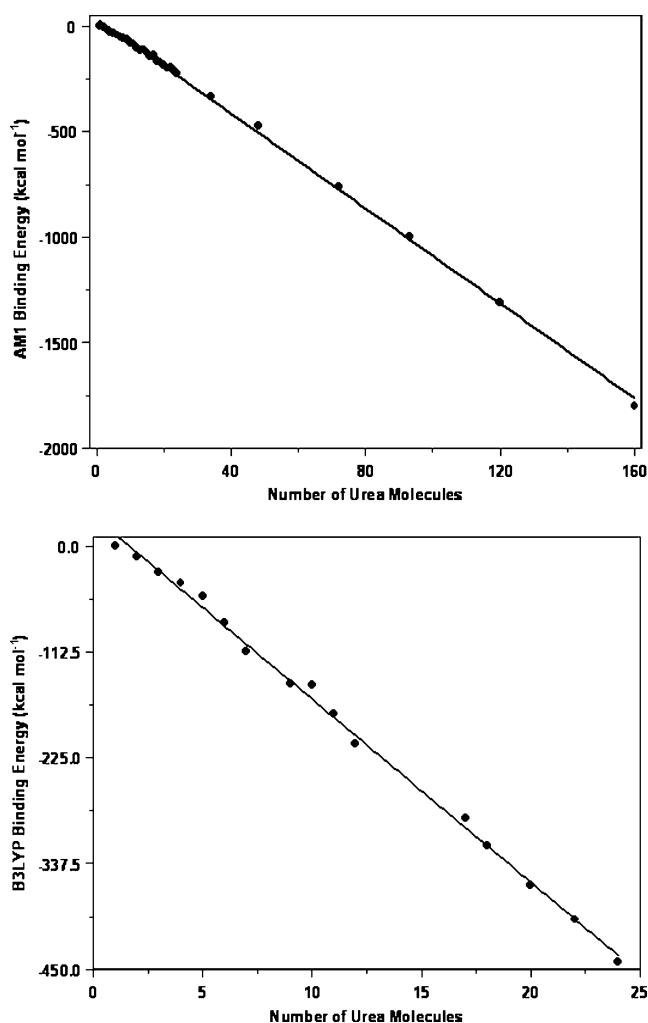


Fig. 7 Calculated AM1 (*top*) and B3LYP (*bottom*) binding energies (kcal mol⁻¹) of urea clusters

The calculated and experimental lattice constants are listed in Table 6. Swaminathan et al. [13] investigated the crystal structure and molecular thermal motion of urea and observed that the lattice parameters, especially the lattice parameter *a*, change significantly with increasing temperature because of the hydrogen bonding. One can see that AM1 agrees better with experiment for the *c* lattice vector than for the *a* lattice vector. Very satisfactory

performance is observed for B3LYP with an acceptable mean deviation.

The force field

The computed RESP charges for each dimer are listed in Table 7. Bertran et al. [65] also computed a charge set for nonplanar urea that is similar to ours. The OPLS (optimized potentials for liquid simulations) urea charge set developed by Jorgensen et al. [66] and a modification to the OPLS charges by Nilsson et al. [27] are also shown.

Interaction energies

The geometry of each urea dimer was optimized using force fields based on each RESP charge set. Dimer stability orders were found to agree with those of the CCSD method. The interaction energies computed using the RESP-D3 charge set agree best with the MP2/aug-cc-pVTZ energies (Table 8). Therefore, we used this charge set for further calculations. Nonbonding interaction parameters from both GAFF and OPLS (Table 9) were tested for energy minimizations of the linear dimer that is found in the crystal structure. Figure 8 shows the linear dimer geometries obtained and Table 10 shows the parameters used in the energy minimization of each structure.

The linear dimer **a** (Fig. 8) is the geometry obtained from MP2 optimization. The dimer **b** was obtained from energy minimization with unmodified GAFF [29] parameters. The C=O and C–N bond distances are far smaller than the diffraction results (1.243 Å [7] and 1.335 Å [6]). Changing only the bond and angle parameters to those given by Cornell et al. [57] gave structure **c**, in which the bond distances are in very good agreement with the neutron diffraction results. The deviations from experiment are only 0.012, 0.004, and 0.004 Å for the C=O, C–N, and N–H bonds, respectively. Using the nonbonding interaction parameters from OPLS led to a large change in the hydrogen-bond distances (Fig. 8, **d–f**). The experimental hydrogen bond length [5] varies between 2.014 and 2.071 Å. The GAFF nonbonding parameters underestimate these limits by 0.045 and 0.102 Å, whereas OPLS parameters overestimate them seriously (by 2.478 and 2.421 Å, respectively).

Table 6 A comparison of the lattice constants (given in Å) calculated by B3LYP and AM1 with experimental data. Percentage deviations with respect to experimental values obtained by Zavodnik et al. [5] are reported in parentheses

	12K [13]	30K [13]	60K [13]	90K [13]	123K [13]	150K [13]	173K [13]	293K [5]	298K [12]	AM1	B3LYP
<i>a</i>	5.565	5.565	5.570	5.576	5.584	5.590	5.598	5.660	5.662	5.481 (–3.27)	5.606 (–0.96)
<i>c</i>	4.684	4.685	4.688	4.689	4.689	4.692	4.694	4.711	4.716	4.683 (–0.60)	4.747 (0.76)
<i>c/a</i>	0.8417	0.8419	0.8417	0.8409	0.8397	0.8394	0.8385	0.8323	0.8329	0.8544	0.8468

Table 7 RESP charges calculated with MP2/aug-cc-pVDZ for each dimer structure

	RESP-D1	RESP-D2	RESP-D3	RESP-D4	RESP-D5	RESP-D6	RESP-D7	Bertran et al. [65]	Nilsson et al. [27]	OPLS [66]
C	1.172	0.675	0.884	0.783	0.893	0.866	0.871	0.963	0.142	0.142
O	-0.795	-0.571	-0.660	-0.600	-0.622	-0.614	-0.653	-0.578	-0.502	-0.390
N	-1.098	-0.735	-0.888	-0.777	-0.888	-0.880	-0.873	-1.004	-0.569	-0.542
H	0.454	0.342	0.388	0.343	0.376	0.377	0.382	0.406	0.333	0.333

Table 8 Interaction energies (kcal mol⁻¹) of urea dimers

	MP2		CCSD	Force field ^c , RESP charge set						
	aug-cc-pVDZ ^a	aug-cc-pVTZ ^b	aug-cc-pVDZ ^b	D1	D2	D3	D4	D5	D6	D7
D1	-10.33	-9.58	-9.93	-16.07	-9.86	-11.99	-9.83	-10.38	1.62	-11.76
D2	-12.04	-10.79	-11.71	-11.7	-7.79	-8.86	-7.51	-7.54	4.44	-8.73
D3	-16.14	-14.75	-15.37	-17.33	-11.12	-13.12	-10.77	-11.41	0.49	-12.86
D4	-10.42	-8.72	-9.80	-6.47	-4.45	-4.77	-4.12	-4.35	7.56	-4.76
D5	-12.83	-10.81	-11.93	-6.86	-2.74	-3.03	-2.58	-2.61	9.39	-2.85
D6	-17.89	-16.97	-17.43	-19.37	-12.18	-14.62	-11.95	-12.62	-0.68	-14.34
D7	-16.09	-14.72	-15.34	-17.36	-11.18	-13.16	-10.8	-11.44	0.45	-12.9

^aBasis set corrected energy.

^bSingle-point energy at the MP2/aug-cc-pVDZ geometry.

^cTotal interaction energy.

We therefore decided to use parameter set **c** for further work. The complete parameter set is defined in Table 11.

The calculated lattice energy for urea using this force field is 23.9 kcal mol⁻¹. This agrees well with the experimental sublimation energies of -20.95±0.21 [63] and -23.6 kcal mol⁻¹ [64]. The calculated lattice constants ($a=5.488$, $c=4.611$, and $c/a=0.8402$) tend to be slightly

shorter than the experimental values [13] ($a=5.565$, $c=4.684$, and $c/a=0.8417$), but the mean deviations of -1.40 and -1.58%, respectively, are acceptable considering that the force field was constructed from data for dimers.

Summary and conclusions

We have optimized the force field for urea to reproduce the observed molecular geometries and structures of urea dimers. The resulting force field gives good results for the urea crystal and the force field should thus be well suited to calculations of the nucleation and dissolution of urea crystals and clathrates. We will report such studies using the new force field for molecular dynamics simulations.

The quantum mechanical calculations show that B3LYP gives a reasonable lattice energy for urea, whereas AM1 underestimates it significantly. The former suggests that dispersion is not very important for crystalline urea.

Table 9 Nonbonding interaction parameters; ϵ in kcal mol⁻¹ is the depth of the potential well and σ (Å) is the distance at which the *inter*-particle potential is zero

	GAFF		OPLS	
	σ	ϵ	σ	ϵ
C	1.908	0.086	3.750	0.105
O	1.661	0.210	2.960	0.210
N	1.824	0.170	3.250	0.170
H	0.600	0.016	0.000	0.000

Fig. 8 Linear dimer geometries (distances in Å) after energy minimization with the different force-field parameter sets defined in Table 10. The distances given in *italics* are the C...C distances

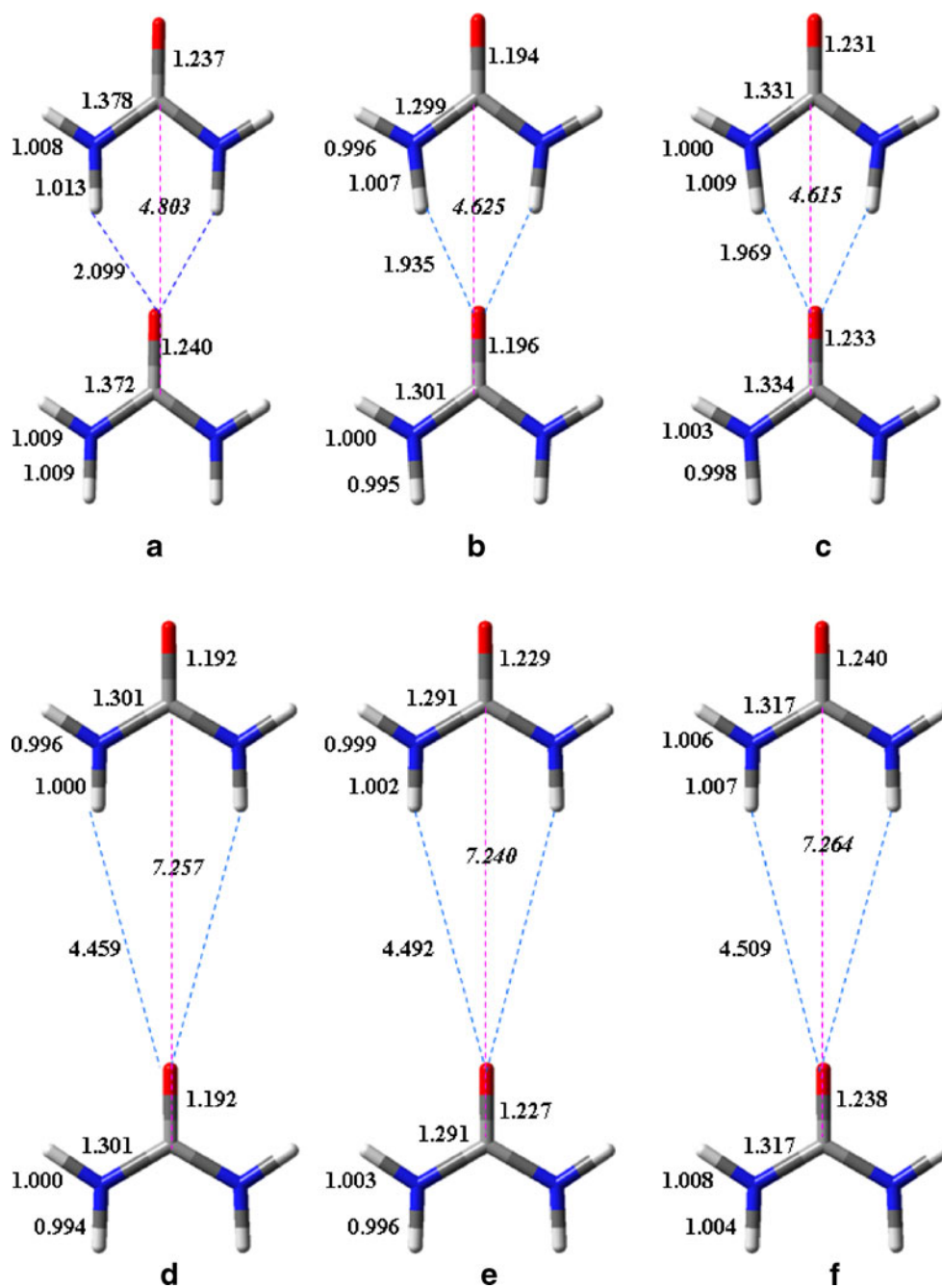


Table 10 The parameters used for energy minimization of the linear dimer

	Bond and angle parameters	Nonbonding interaction parameters	Charge parameters
b	GAFF	GAFF	Resp-D3
c	Cornell et al.	GAFF	Resp-D3
d	GAFF	OPLS	Resp-D3
e	Cornell et al.	OPLS	Resp-D3
f	Cornell et al.	OPLS	OPLS

Table 11 Improved general AMBER force field parameters

Bond parameters				
Bond	K_r^a	r^b		
C–O	656	1.250		
C–N	424	1.383		
HN–N	434	1.010		
Angle parameters				
Angle	K_θ^c	θ^d		
N–C–O	80	120.9		
C–N–HN	30	120.0		
HN–N–HN	35	120.0		
N–C–N	70	118.6		
Dihedral parameters				
Torsion	No. of paths ^e	$V_n/2^f$	γ^g	n^h
HN–N–C–O	1	2.5	180	–2
HN–N–C–O	1	2.0	0	1
Improper dihedral parameters				
Torsion		$V_n/2^f$	γ^g	n^h
N–N–C–O		10.5	180	2
C–HN–N–HN		1.1	180	2
Nonbonding parameters				
Atom type	σ (Å)	ϵ (kcal mol ^{–1})		
HN	0.6000	0.0157		
O	1.6612	0.2100		
C	1.9080	0.0860		
N	1.8240	0.1700		

^a Force constant (kcal mol^{–1} Å^{–2}). ^b Bond distance (Å).

^c Force constant (kcal mol^{–1} radian^{–2}). ^d Angle (°).

^e Number of bond paths that the total $V_n/2^f$ is divided into.

^f Magnitude of torsion (kcal mol^{–1}).

^g Phase offset (°).

^h The periodicity of the torsion. A negative value is not used in the computation but signifies more than one component around a given bond.

Acknowledgments This work was supported by the Deutsche Forschungsgemeinschaft as part of the project PE 42710-2 and the Excellence Cluster *Engineering of Advanced Materials*. We also thank Matthias Hennemann, Christof Jäger and Frank Beierlein for their support.

References

- Bonin M, Marshall WG, Weber HP, Tolendo P (1999) Polymorphism in urea. IOP Publishing, Philadelphia. <http://www.isis.rl.ac.uk/archive/isis99/highlights/urea4.htm>. Accessed August 1999
- Mathews CK, van Holde KE (1996) Biochemistry, 2nd edn. Benjamin Cummings, Menlo Park, p 4
- Bhatnagar VM (1968) Clathrates of urea nad thiourea. J Struct Chem 8:513–529. doi:10.1007/BF00751656
- Theophanides T, Harvey PD (1987) Structural and spectroscopic properties of metal–urea complexes. Coord Chem Rev 76:237–264. doi:10.1016/0010-8545(87)85005-1
- Zavodnik V, Stash A, Tsirelson V, De Vires R, Feil D (1999) Electron density study of urea using TDS-corrected X-ray diffraction data: quantitative comparison of experimental and theoretical results. Acta Crystallogr Sect B 55:45–54. doi:10.1107/S0108768198005746
- Vaughan P, Donohue J (1952) The structure of urea. Interatomic distances and resonance in urea and related compounds. Acta Crystallogr 5:530–535. doi:10.1107/S0365110X52001477
- Worsham JE, Levy HA, Peterson SE (1957) The positions of hydrogen atoms in urea by neutron diffraction. Acta Crystallogr 10:319–323. doi:10.1107/S0365110X57000924
- Andrew ER, Hyndman D (1953) Proton magnetic resonance evidence for the planar structure of the urea molecule. Proc Phys Soc A66:1187–1188. doi:10.1088/0370-1298/66/12/119
- Wyckoff RWG (1930) Z Kristallogr 75:529–537
- Hendriks SB (1928) The crystal structure of urea and the molecular symmetry of thiourea. J Am Chem Soc 50:2455–2464. doi:10.1021/ja01396a019
- Mark H, Weissenberg K (1923) Röntgenographische Bestimmung der Struktur des Harnstoffs und des Zinntetrahydrids. Z Phys 16:1–22. doi:10.1007/BF01327372
- Sklar N, Senko ME, Post B (1961) Thermal effects in urea: the crystal structure at –140 °C and at room temperature. Acta Crystallogr 14:716–722. doi:10.1107/S0365110X61002187
- Swaminathan S, Craven BM (1984) The crystal structure and molecular thermal motion of urea at 12, 60 and 123 K from neutron diffraction. Acta Crystallogr Sect B 40:300–306. doi:10.1107/S0108768184002135
- Pluta T, Sadlej AJ (2001) Electric properties of urea and thiourea. J Chem Phys 114:136–146. doi:10.1063/1.1328398
- Alparone A, Millefiori S (2005) Gas and solution phase electronic and vibrational (hyper)polarizabilities in the series formaldehyde, formamide and urea: CCSD(T) and DFT theoretical study. Chem Phys Lett 416:282–288
- Olah GA, Surya Prakash GK, Rasul G (2008) ¹³C and ¹⁵N NMR and ab initio/GIAO-CCSD(T) study of the structure of mono-, di-, and triprotonated guanidine, urea, and thiourea. J Phys Chem C 112:7895–7899. doi:10.1021/jp711727c
- Benková Z, Černušák I, Zahradník P (2007) Electric properties of formaldehyde, thioformaldehyde, urea, formamide, and thioformamide: post-HF and DFT study. Int J Quantum Chem 107:2133–2152. doi:10.1002/qua.21399
- Masunov A, Dannenberg JJ (1999) Theoretical study of urea. I. Monomers and dimers. J Phys Chem A 103:178–184. doi:10.1021/jp9835871
- Spoliti M, Perrone G, Bencivenni L, Pieretti A, Grandi A, Ramondo F (2005) Computational and vibrational spectroscopy study of the microclusters of C₂ symmetry urea molecule in the ¹A electronic ground state. J Mol Struct 756:113–126. doi:10.1016/j.theochem.2005.07.021
- Singh A, Chakraborty S, Ganguly B (2007) Computational study of urea and its homologue glycineamide: conformations, rotational barriers, and relative interactions with sodium chloride. Langmuir 23:5406–5411. doi:10.1021/la062405o
- Civalleri B, Doll K, Zicovich-Wilson CM (2007) Ab initio investigation of structure and cohesive energy of crystalline urea. J Phys Chem B 111:26–33. doi:10.1021/jp065757c
- Boek ES, Briels WJ (1993) Molecular dynamics simulations of aqueous urea solutions: study of dimer stability and solution structure, and calculation of the total nitrogen radial distribution function G_N(r). J Chem Phys 98:1422–1427. doi:10.1063/1.464306
- Astrand PO, Wallqvist A, Karlström G (1994) Molecular dynamics simulations of 2 m aqueous urea solutions. J Phys Chem 98:8224–8233. doi:10.1021/j100084a046

24. Boek ES, Briels WJ, van Eerden J, Feil D (1992) Molecular-dynamics simulations of interfaces between water and crystalline urea. *J Chem Phys* 96:7010–7018. doi:10.1063/1.462560
25. Liu XY, Boek ES, Briels WJ, Bennema P (1995) Analysis of morphology of crystals based on identification of interfacial structure. *J Chem Phys* 103:3747–3754. doi:10.1063/1.470053
26. Kallies B (2002) Coupling of solvent and solute dynamics—molecular dynamics simulations of aqueous urea solutions with different intramolecular potentials. *Phys Chem Chem Phys* 4:86–95. doi:10.1039/b105836n
27. Caballo-Herrera A, Nilsson L (2006) Urea parametrization for molecular dynamics simulations. *J Mol Struct Theochem* 758:139–148. doi:10.1016/j.theochem.2005.10.018
28. Etter M (1990) Encoding and decoding hydrogen-bond patterns of organic compounds. *Acc Chem Res* 23:120–126. doi:10.1021/ar00172a005
29. Wang J, Wolf RM, Caldwell JW, Kollman PA, Case DA (2004) Development and testing of a general amber force field. *J Comput Chem* 25:1157–1174. doi:10.1002/jcc.20035
30. Clark T, Alex A, Beck B, Burkhardt F, Chandrasekhar J, Gedeck P, Horn A, Hutter M, Martin B, Rauhut G, Sauer W, Schindler T, Steinke T (2003) VAMP v.10.0. Accelrys Inc., San Diego
31. Frisch MJ, Trucks GW, Schlegel HB, Scuseria GE, Robb MA, Cheeseman JR, Montgomery JA Jr, Vreven T, Kudin KN, Burant JC, Millam JM, Iyengar SS, Tomasi J, Barone V, Mennucci B, Cossi M, Scalmani G, Rega N, Petersson GA, Nakatsuji H, Hada M, Ehara M, Toyota K, Fukuda R, Hasegawa J, Ishida M, Nakajima T, Honda Y, Kitao O, Nakai H, Klene M, Li X, Knox JE, Hratchian HP, Cross JB, Bakken V, Adamo C, Jaramillo J, Gomperts R, Stratmann RE, Yazyev O, Austin AJ, Cammi R, Pomelli C, Ochterski JW, Ayala PY, Morokuma K, Voth GA, Salvador P, Dannenberg JJ, Zakrzewski VG, Dapprich S, Daniels AD, Strain MC, Farkas O, Malick DK, Rabuck AD, Raghavachari K, Foresman JB, Ortiz JV, Cui Q, Baboul AG, Clifford S, Cioslowski J, Stefanov BB, Liu G, Liashenko A, Piskorz P, Komaromi I, Martin RL, Fox DJ, Keith T, Al-Laham MA, Peng CY, Nanayakkara A, Challacombe M, Gill PMW, Johnson B, Chen W, Wong MW, Gonzalez C, Pople JA (2004) Gaussian 03, revision D.02. Gaussian, Inc., Wallingford
32. Čížek J (1969) In: Lefebvre R, Moser C (eds) Correlation effects in atoms & molecules. *Advances in chemical physics* 14. Interscience, New York, pp 35
33. Purvis GD, Bartlett RJ (1982) A full coupled-cluster singles and doubles model: the inclusion of disconnected triples. *J Chem Phys* 76:1910–1918. doi:10.1063/1.443164
34. Scuseria GE, Janssen CL, Schaefer HF III (1988) An efficient reformulation of the closed-shell coupled cluster single and double excitation (CCSD) equations. *J Chem Phys* 89:7382–7387. doi:10.1063/1.455269
35. Moller C, Plesset MS (1934) Note on an approximation treatment for many-electron systems. *Phys Rev* 46:618–622. doi:10.1103/PhysRev.46.618
36. Becke AD (1993) Density-functional thermochemistry. III. The role of exact exchange. *J Chem Phys* 98:5648–5652. doi:10.1063/1.464913
37. Lee C, Yang W, Parr RG (1988) Development of the Colle–Salvetti correlation-energy formula into a functional of the electron density. *Phys Rev B* 37:785–789. doi:10.1103/PhysRevB.37.785
38. Dewar M, Thiel W (1977) Ground states of molecules. 38. The MNDO method. Approximations and parameters. *J Am Chem Soc* 99:4899–4907. doi:10.1021/ja00457a004
39. Nyden MR, Petersson GA (1981) Complete basis set correlation energies. I. The asymptotic convergence of pair natural orbital expansions. *J Chem Phys* 75:1843–1862. doi:10.1063/1.442208
40. Petersson GA, Al-Laham MA (1991) A complete basis set model chemistry. II. Open-shell systems and the total energies of the first-row atoms. *J Chem Phys* 94:6081–6090. doi:10.1063/1.460447
41. Petersson GA, Tensfeldt TG, Montgomery JA Jr (1991) A complete basis set model chemistry. III. The complete basis set-quadratic configuration interaction family of methods. *J Chem Phys* 94:6091–6101. doi:10.1063/1.460448
42. Dunning TH Jr (1989) Gaussian basis sets for use in correlated molecular calculations. I. The atoms boron through neon and hydrogen. *J Chem Phys* 90:1007–1023. doi:10.1063/1.456153
43. Kendall RA, Dunning TH Jr, Harrison RJ (1992) Electron affinities of the first-row atoms revisited. Systematic basis sets and wave functions. *J Chem Phys* 96:6796–6806. doi:10.1063/1.462569
44. Woon DE, Dunning TH Jr (1993) Gaussian-basis sets for use in correlated molecular calculations. 3. The atoms aluminum through argon. *J Chem Phys* 98:1358–1371. doi:10.1063/1.464303
45. Peterson KA, Woon DE, Dunning TH Jr (1994) Benchmark calculations with correlated molecular wave functions. IV. The classical barrier height of the $H+H_2 \rightarrow H_2+H$ reaction. *J Chem Phys* 100:7410–7415. doi:10.1063/1.466884
46. Wilson AK, van Mourik T, Dunning TH Jr (1996) Gaussian basis sets for use in correlated molecular calculations. VI. Sextuple zeta correlation consistent basis sets for boron through neon. *J Mol Struct* 388:339–349. doi:10.1016/S0166-1280(96)80048-0
47. McLean AD, Chandler GS (1980) Contracted Gaussian-basis sets for molecular calculations. 1. 2nd row atoms, $Z=11-18$. *J Chem Phys* 72:5639–5648. doi:10.1063/1.438980
48. Raghavachari K, Binkley JS, Seeger R, Pople JA (1980) Self-consistent molecular orbital methods. 20. Basis set for correlated wave-functions. *J Chem Phys* 72:650–654. doi:10.1063/1.438955
49. Clark T, Chandrasekhar J, Spitznagel GW, Pvr S (1983) Efficient diffuse function-augmented basis-sets for anion calculations. 3. The 3-21+G basis set for 1st-row elements, Li-F. *J Comput Chem* 4:294–301. doi:10.1002/jcc.540040303
50. Ditchfield R, Hehre WJ, Pople JA (1971) Self-consistent molecular orbital methods. 9. Extended Gaussian-type basis for molecular-orbital studies of organic molecules. *J Chem Phys* 54:724–728. doi:10.1063/1.1674902
51. Frisch MJ, Pople JA, Binkley JS (1984) Self-consistent molecular orbital methods. 25. Supplementary functions for Gaussian basis sets. *J Chem Phys* 80:3265–3269. doi:10.1063/1.447079
52. Boys SF, Bernardi F (1970) The calculation of small molecular interactions by the differences of separate total energies. Some procedures with reduced errors. *Mol Phys* 19:553–566. doi:10.1080/00268977000101561
53. Case DA, Darden TA, Cheatham TE III, Simmerling CL, Wang J, Duke RE, Luo R, Crowley M, Walker RC, Zhang W, Merz KM, Wang B, Hayik S, Roitberg A, Seabra G, Kolossváry I, Wong KF, Paesani F, Vanicek J, Wu X, Brozell SR, Steinbrecher T, Gohlke H, Yang L, Tan C, Mongan J, Hornak V, Cui G, Mathews DH, Seetin MG, Sagui C, Babin V, Kollman PA (2008) AMBER 10. University of California, San Francisco
54. Bayly CI, Cieplak P, Cornell WD, Kollman PA (1993) A well-behaved electrostatic potential based method using charge restraints for deriving atomic charges: the RESP model. *J Phys Chem* 97:10269–10280. doi:10.1021/j100142a004
55. Brown RD, Godfrey PD, Story J (1975) The microwave spectrum of urea. *J Mol Spectrosc* 58:445–450. doi:10.1016/0022-2852(75)90224-6
56. Strassner T (1996) Ab initio and molecular mechanics calculations of various substituted ureas: rotational barriers and a new parametrization for ureas. *J Mol Model* 2:217–226. doi:10.1007/s0089460020217
57. Cornell WD, Cieplak P, Bayly CI, Gould IR, Merz KM Jr, Ferguson DM, Spellmeyer DC, Fox T, Caldwell JW, Kollman PA (1995) A second generation force field for the simulation of

- proteins, nucleic acids, and organic molecules. *J Am Chem Soc* 117:5179–5197. doi:10.1021/ja00124a002
58. Gilkerson W, Srivastava K (1960) The dipole moment of urea. *J Phys Chem* 64:1485–1487. doi:10.1021/j100839a032
59. Lefebvre J (1973) Longitudinal phonons of translation along the 4 axis on urea. *Solid State Commun* 13:1873–1875. doi:10.1016/0038-1098(73)90748-5
60. Lee JS (1999) On the effectiveness of function counterpoise method in the calculation of He–He interaction energies. *Bull Korean Chem Soc* 20:241–243
61. Schwenke DW, Truhlar DG (1985) Systematic study of basis set superposition errors in the calculated interaction energy of two HF molecules. *J Chem Phys* 85:2418–2426. doi:10.1063/1.448335
62. Åstrand PO, Wallqvist A, Karlström G (1994) Nonempirical intermolecular potentials for urea–water systems. *J Chem Phys* 100:1262–1273. doi:10.1063/1.466655
63. Suzuki K, Onishi S, Koide T, Seki S (1956) Vapor pressures of molecular crystals. XI. Vapor pressures of crystalline urea and diformylhydrazine. Energies of hydrogen bonds in these crystals. *Bull Chem Soc Jpn* 29:127–131. doi:10.1246/bcsj.29.127
64. Dewit HGM, Van Miltenburg JC, DeKruif CG (1983) Thermodynamic properties of molecular organic crystals containing nitrogen, oxygen, and sulphur 1. Vapour pressures and enthalpies of sublimation. *J Chem Thermodyn* 15:651–663. doi:10.1016/002-9614(83)90079-4
65. Bertran CA, Cirino JJV, Freitas LCG (2002) Theoretical studies of concentrated aqueous urea solutions using computational Monte Carlo simulation. *J Braz Chem Soc* 13:238–244. doi:10.1590/S0103-50532002000200016
66. Duffy EM, Severance DL, Jorgensen WL (1993) Urea: potential functions, log P, and free energy of hydration. *Isr J Chem* 33:323–330